Pergamon

Tetrahedron 57 (2001) 3657–3671

TETRAHEDRON

Conjugated macrocycles related to the porphyrins. Part 18:☆ Synthesis and spectroscopic characterization of electron-rich benzi- and oxybenziporphyrins: influence of steric and electronic factors on porphyrinoid aromaticity

Daniel T. Richter and Timothy D. Lash*

Department of Chemistry, Illinois State University, Normal, IL 61790-4160, USA

Received 2 October 2000; accepted 30 November 2000

Abstract—Although 4,6-dihydroxyisophthalaldehydes failed to condense with tripyrranes to produce porphyrinoid products, the related dimethoxydialdehydes reacted with tripyrrane **9** to give, following oxidation with aqueous ferric chloride solution, nonaromatic dimethoxybenziporphyrins **20** in excellent yields. In the presence of TFA, dications were generated that showed weakly diatropic properties by proton NMR spectroscopy. This observation was attributed to the ability of the methoxy units to facilitate charge delocalization. Treatment of **20** with 50 equiv. of boron tribromide cleaved one of the methyl ethers to produce the related methoxyoxybenziporphyrins **24**. These porphyrinoids showed strong diamagnetic ring currents due to the presence of 18 π-electron delocalization pathways within these structures. On treatment with TFA, the resulting dications show significantly reduced ring currents although their diatropic character is retained to a far greater extent than when the methoxy substituents are absent. For both **20** and **24**, the methoxy groups are more effective at charge delocalization, which results in increased diatropicity, when there is no adjacent alkyl substituent. Treatment of **20a** with HBr in refluxing acetic acid cleaved both methyl ethers to give the highly insoluble hydroxyoxybenziporphyrin **17**. Although the spectroscopic properties of the free base could not be assessed, this compound was soluble in TFA–chloroform and the resulting dication proved to be highly aromatic as judged by NMR and UV–vis spectroscopy. Treatment of the **20b** with HBr–acetic acid again cleaved both methyl ethers but also gave an unexpected oxidation to give a diketone bearing a 3° alcohol unit. This novel porphyrinoid retains an 18 π-delocalization pathway, shows porphyrin-like UV–vis spectra and is highly diatropic as the free base and in protonated form as judged by proton NMR spectroscopy.

1. Introduction

The porphyrin macrocycle **1** has long been recognized as a fully π-delocalized aromatic system. The proton NMR spectra for porphyrins are particularly diagnostic showing powerful diamagnetic ring currents with the internal NH's shifted upfield to, approximately, −4 ppm while the external bridge methines (*meso*-protons) are generally downfield near +10 ppm.[2] Porphyrins also have very characteristic electronic absorption spectra dominated by a 'Soret' band near 400 nm ($\epsilon \approx 2\times10^5$), followed by four smaller 'Q bands' between 490 and 650 nm.[3] Free base porphyrins consist of two rapidly interconverting tautomers **1a** and **1b**, with minor contributions from less favored '*cis*' tautomers such as **1c** (Chart 1)).[3] In each of these structures, an 18π electron delocalization pathway (shown in bold) can be discerned and for this reason porphyrins are often considered to be the bridged [18]annulenes of Nature.[4,5] Protonation of the inner nitrogens does not disrupt the aromatic properties of the porphyrin macrocycle, and if anything enhances its diatropicity, and metallation of the inner core does not significantly disrupt macrocyclic aromaticity.[3] While the presence of closed 18π electron pathways provides an explanation for the aromatic properties of porphyrins, the nitrogen atoms clearly have a significant impact as well. In a recent paper,[6] Schleyer has proposed that the aromatic properties of porphyrins are best described as 22π-electron delocalized systems that utilize two of the nitrogen electron pairs (structure **2**). Both descriptions can equally well be applied to related systems such as the porphyrin isomer Porphycene (**3**).[7]

In order to gain a better understanding of porphyrinoid aromaticity, many examples of related macrocyclic systems have been synthesized including porphyrin isomers[8] and expanded porphyrins.[9] Replacement of one or more of the pyrrole subunits with other ring systems potentially allows the function of the nitrogen atoms to be rationally assessed.[10] Early studies were directed towards the synthesis

☆ For Part 17 see Ref. 1.

Keywords: carbaporphyrinoid; benziporphyrn; aromaticity; tautomerization; macrocycles.

* Corresponding author. Tel.: +1-309-438-8554; fax: +1-309-438-5538; e-mail: tdlash@ilstu.edu

0040–4020/01/$ - see front matter
PII: S0040-4020(01)00256-3

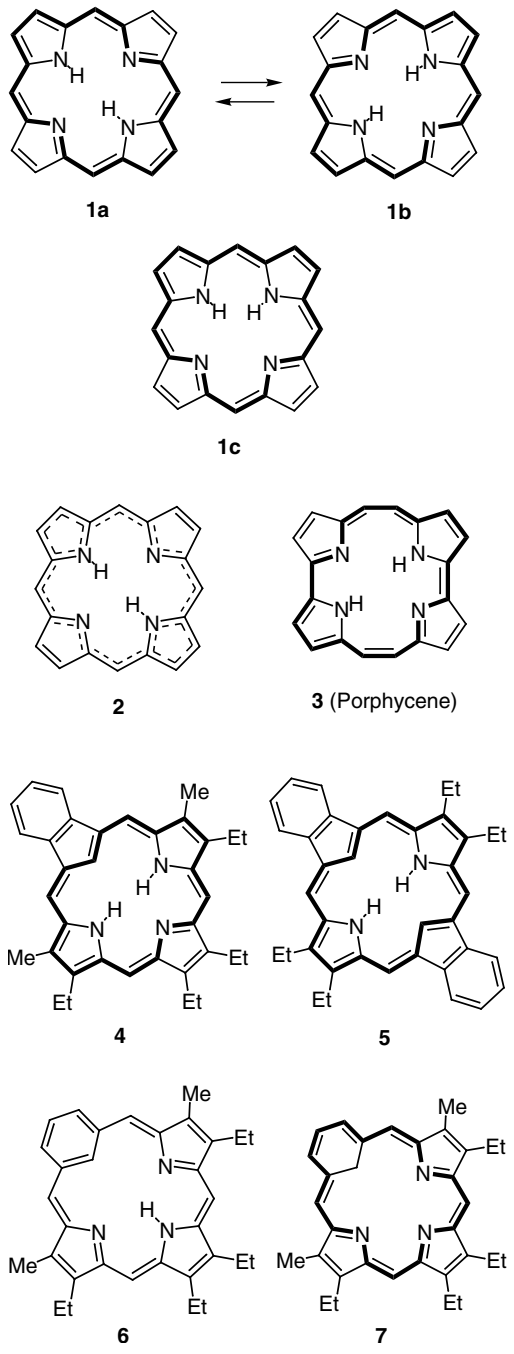

Chart 1.

of porphyrin analogues with furan, thiophene, selenophene or tellurophene rings,[11] but the presence of the chalconide elements provides a substitute for the nitrogen electron pairs. The incorporation of carbocyclic rings into porphyrin analogue structures has only been accomplished fairly recently.[12,13] For instance, carbaporphyrins (e.g. **4**)[14] and dicarbaporphyrin **5**[5] have been reported to retain macrocyclic aromaticity, while benziporphyrin **6** behaves as a nonaromatic system overall.[16,17] In the latter case, one can imagine the existence of a fully aromatic tautomer **7** but this arrangement can only exist at the expense of losing the benzene subunit's aromatic properties. In this case, the competition between 6-π arene and porphyrinoid

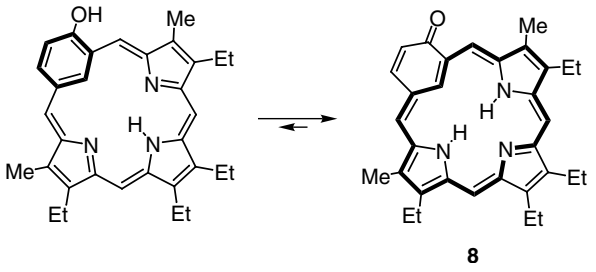

Scheme 1.

aromaticity greatly favors the former but other factors can influence the outcome of these competitive relationships.[12,17]

In an earlier study, we demonstrated that the addition of a suitably placed hydroxy group to the benziporphyrin system facilitates a 'keto–enol' tautomerization to produce oxybenziporphyrin **8** (Scheme 1),[18] at the time the first example of an aromatic porphyrin analogue with a carbocyclic ring in place of a pyrrole subunit. The synthesis of **8** made use of the so-called '3+1' methodology[19–21] where a tripyrrane **9** was condensed with 5-formylsalicylaldehyde to generate, following an oxidation step with DDQ, the fully aromatic macrocycle **8** (Scheme 2).[18] Unlike benziporphyrin, which shows the internal and external benzene protons between 7.7 and 8.0 ppm,[17] oxybenziporphyrin shows a powerful diamagnetic ring current by proton NMR spectroscopy. The oxybenziporphyrin system may consist of three different tautomers (**8a–c**), although theoretical studies on related carbaporphyrin structures indicate that tautomer **8a** should be favored.[22] If more than one tautomer is present, they must interconvert rapidly on the NMR timescale as only one set of resonances is observed.[17,18] The NH protons show up as a broad signal at −4 ppm, while the internal CH appears as a ^4J coupled doublet near −7 ppm.[18] The exterior protons are similarly deshielded as a result of the porphyrinoid ring current. The porphyrinoid properties are also obvious in the UV–vis spectrum where strong Soret-like bands appear at 428 and 456 nm, while a series of Q bands extend to 698 nm.[17,18] Addition of trace amounts of TFA results in the formation of a monocation that again appears to favor the aromatic tautomer **10** over nonaromatic structures such as **11**. Further addition of acid produces a dication that shows a drastically reduced diamagnetic ring current by proton NMR spectroscopy and a UV–vis spectrum that showed a greatly diminished Soret band.[17,18] These data indicate that the cross-conjugated phenolic canonical form **12b** is favored over the aromatic contributor **12a**, possibly due in part to crowding within the central cavity that may lead to considerable distortion of the macrocycle from planarity (Scheme 2). Similar properties were observed for a series of oxybenziporphyrins with fused aromatic rings (structures **13–15**, Chart 2).[17]

The addition of a hydroxyl unit onto the benziporphyrin nucleus completely changes the properties of this macrocyclic system by 'switching on' the porphyrinoid aromaticity that would otherwise be disfavored. We anticipated that the addition of a second hydroxy group (structure **16**) would further modify the properties of the porphyrin analogues. While only one of the phenolic OH moieties would

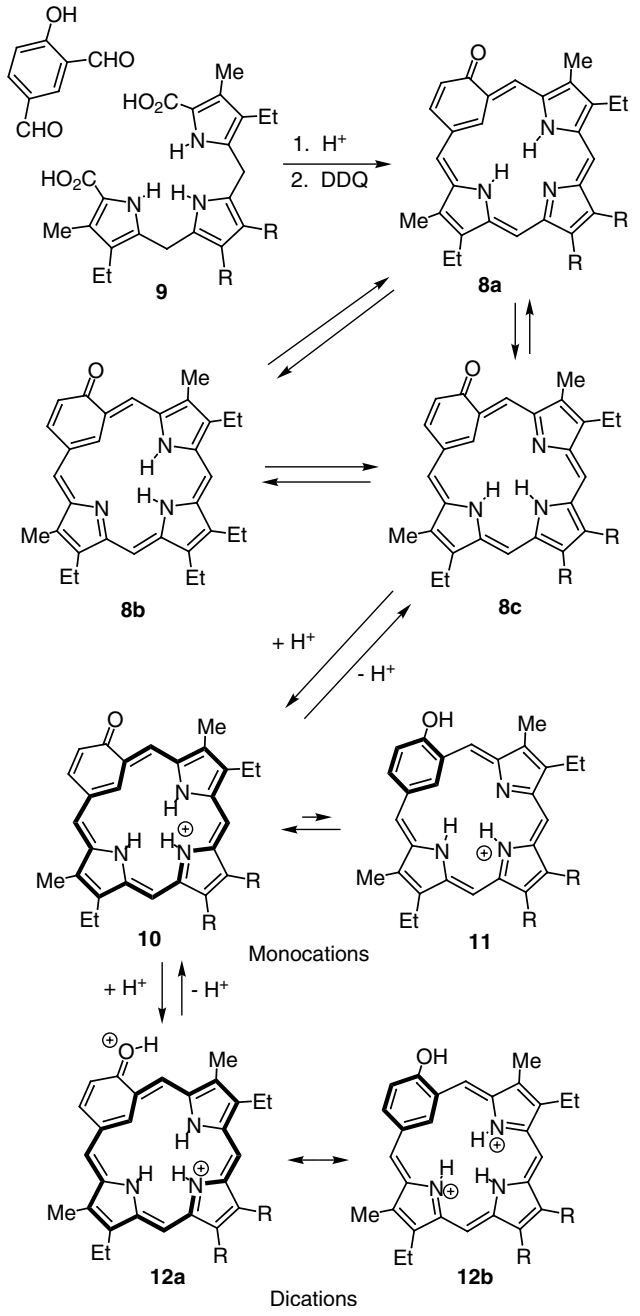

Scheme 2.

be expected to tautomerize to give the keto form (structure **17**), the presence of the remaining electron-donating hydroxyl should significantly alter the properties of these carbaporphyrinoids.[23]

2. Results and discussion

The synthesis of 'dihydroxy' benziporphyrins requires the availability of the related resorcinol derived dialdehydes **18**. These were synthesized in three steps from 1,3-dimethoxybenzene or 2,6-dimethoxytoluene by the established route summarized in Scheme 3.[24] Initially, it was anticipated that dihydroxisophthalaldehyde **18a** would smoothly undergo '3+1' condensation with tripyrrane **9** to produce the

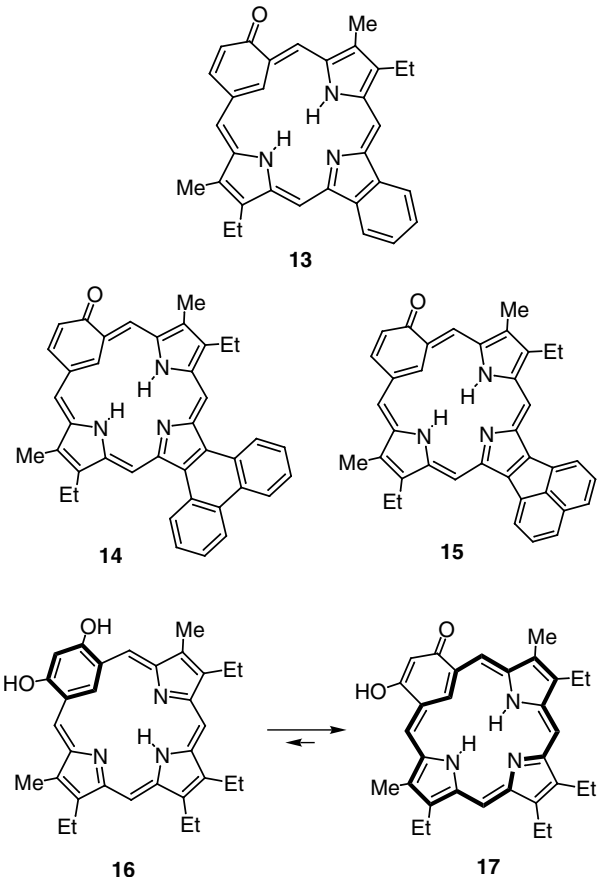

Chart 2.

required hydroxyoxybenziporphyrin **17** (Scheme 4). However, this expectation proved to be elusive. While the related monohydroxydialdehyde gave oxybenziporphyrin **8** in excellent yields, acid catalyzed condensation of **18a** with **9**, followed by oxidation with DDQ or $FeCl_3$,[25] gave only trace amounts of porphyrinoid products. The presence of two strongly electron-donating groups on one side of the

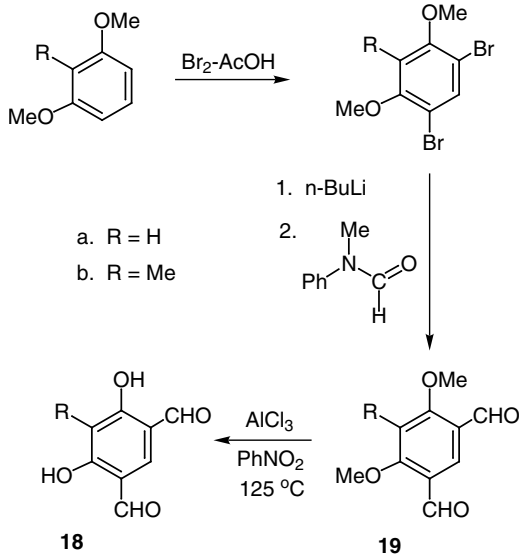

Scheme 3.

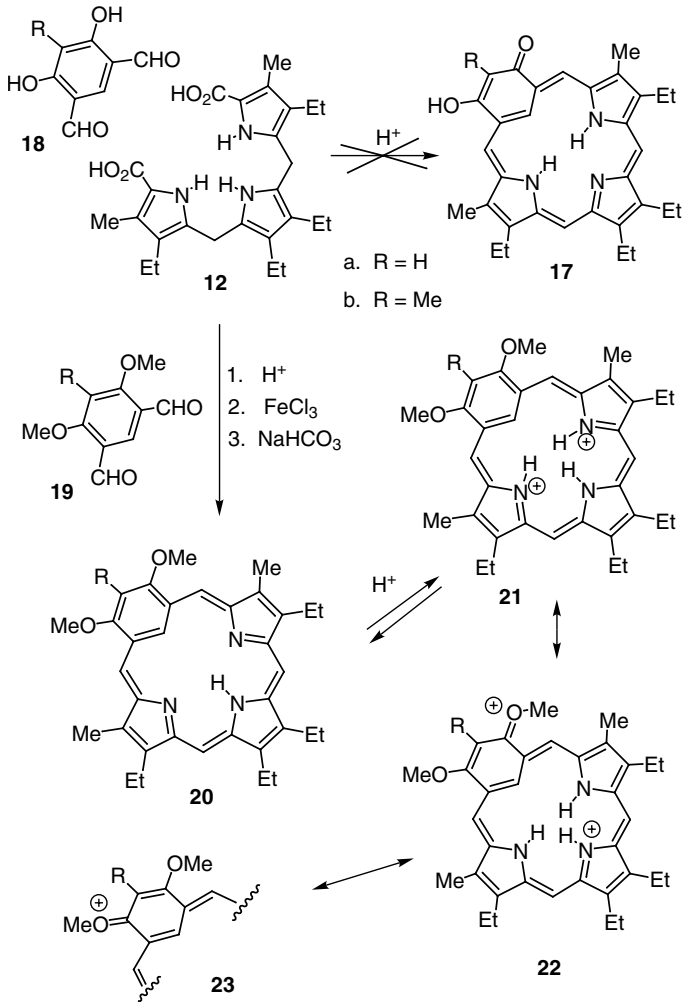

Scheme 4.

benzene precursor may be responsible for unwanted side reactions, and we speculated that these problems might be prevented by blocking off the site between the OH units with a methyl group. Unfortunately, attempts to condense **18b** with **9** also failed to produce isolatable quantities of any macrocyclic products.

This unexpected setback forced us to reconsider our synthetic strategy. The precursors to dihydroxyisophthalaldehydes **18a** and **18b** were the corresponding dimethoxy compounds **19a** and **19b**, respectively (Scheme 3). The lessened electron-donating abilities of the methoxy groups might reduce or circumvent the deleterious effects of the hydroxyl moieties and allow macrocycle formation. However, these condensations would result in the formation of dimethoxybenziporphyrins **20** (Scheme 4) that could not tautomerize to produce aromatic oxybenziporphyrins. While the methoxy groups can be cleaved at a later stage, this approach was initially considered to be far less desirable. Benziporphyrin is a relatively unstable compound and proved to be somewhat difficult to isolate in pure form.[17] The addition of two electron-donating methoxy groups might further increase the reactivity of the ring system making the isolation of these nonaromatic products impractical.

Despite these reservations, the condensation of dimethoxydialdehydes **19a** and **19b** with tripyrrane **9** was carried out under conventional acid catalyzed conditions, followed by oxidation with aqueous ferric chloride solutions. Surprisingly, this chemistry worked remarkably well. Condensation of **19a** with **9** gave the dimethoxybenziporphyrin **20a** in 73–80% yields, while **19b** afforded the related macrocycle **20b** in 55% yield (Scheme 4). The success with this approach relied on minimal handling. Both compounds could easily be recrystallized from chloroform–methanol to give pure products without resorting to chromatography.

The spectroscopic properties for dimethoxybenziporphyrins **20** confirmed that they were non-aromatic compounds. For the proton NMR spectrum of **20a** in $CDCl_3$, the *meso*-protons appeared as two 2H singlets at 7.16 and 8.47 ppm, while the inner benzene proton resonated at 5.07 ppm and the external benzene CH gave a broad signal at 6.78 ppm (Fig. 1). These values suggest that a small amount of aromatic character may be a feature for **20a**, although these minor shifts are not present in the NMR spectra for **20b**. However, addition of TFA to the NMR solution of **20a** resulted in a modest aromatic ring current. Specifically, the interior CH shifted upfield to −0.68 ppm while the exterior *meso*-resonances gave two deshielded singlets at 8.44 and

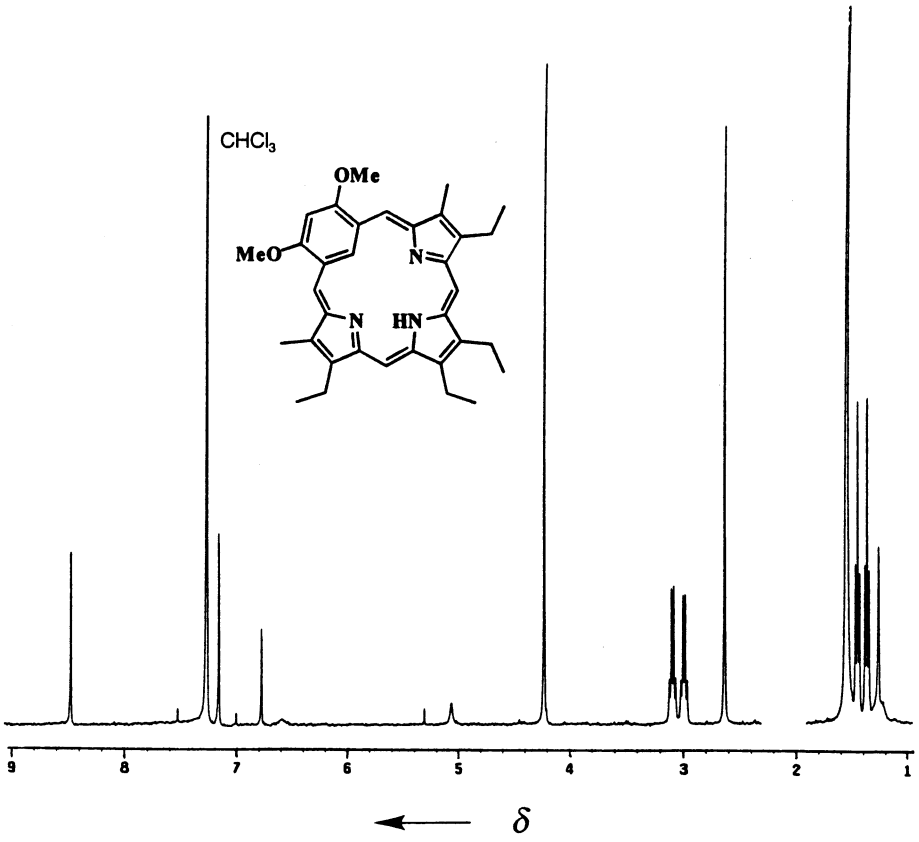

Figure 1. 400 MHz proton NMR spectrum of dimethoxybenziporphyrin **20a** in $CDCl_3$. The free base compound is only sparingly soluble in $CDCl_3$ and this results in the larger than usual solvent impurity peaks.

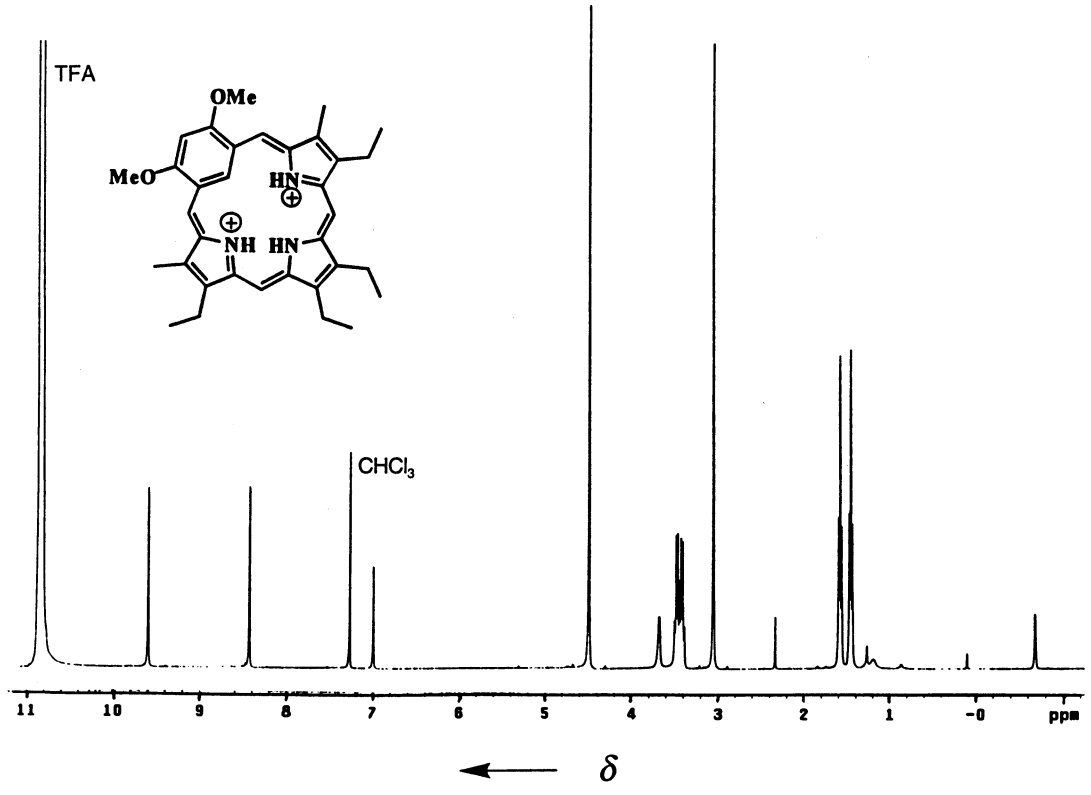

Figure 2. 400 MHz proton NMR spectrum of dimethoxybenziporphyrin **20a** in TFA–$CDCl_3$ showing the emergence of some porphyrinoid aromatic character.

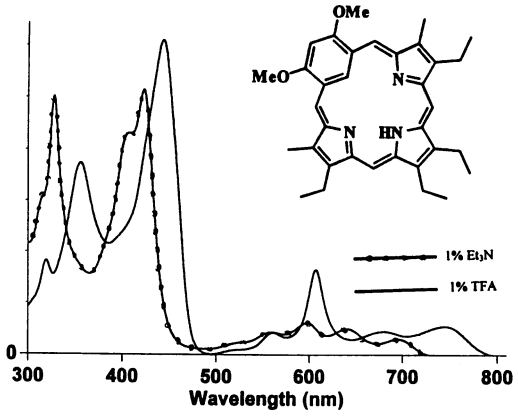

Figure 3. UV–vis spectra of dimethoxybenziporphyrin **20a** in 1% Et_3N–chloroform (dotted line) and 1% TFA–chloroform (solid line).

9.60 ppm (Fig. 2). Further, the methyl substituents shift from 2.63 ppm in the free base to 3.05 ppm in the diprotonated structure. The emergence of a diatropic ring current for dication **21a** is most likely due to favorable charge delocalization. Resonance contributors **22a** and **23a** (Scheme 4) can aid in the delocalization of positive charge while at the same time providing the 18π-electron delocalization pathways for porphyrinoid aromatic character. These profound changes to the electronic characteristics for dimethoxybenziporphyrin **20a** upon protonation can also be seen in the UV–vis spectra. In 1% triethylamine–chloroform, the free base **20a** shows multiple absorptions between 300 and 700 nm, but in 1% TFA–chloroform a Soret-like band emerges at 443 nm ($\log_{10}\epsilon$=4.86) (Fig. 3). However, this phenomenon is rather muted in the case of **20b**. In the proton NMR spectrum, relatively minor shifts are observed (protonation naturally leads to some downfield shifts) although the internal CH still resonates upfield at +2.8 ppm. The UV–vis spectrum in 1% TFA–chloroform is also less porphyrin-like and fails to show a significant Soret-like absorption, although a broad band at 425 nm ($\log_{10}\epsilon$=4.79) is present (Fig. 4). The presence of a methyl group between the two methoxy units leads to steric crowding and this undoubtedly leads to the observed differences. In order for charge delocalization to favor partial porphyrin-type aromatic character, the methoxy oxygens must be sp^2

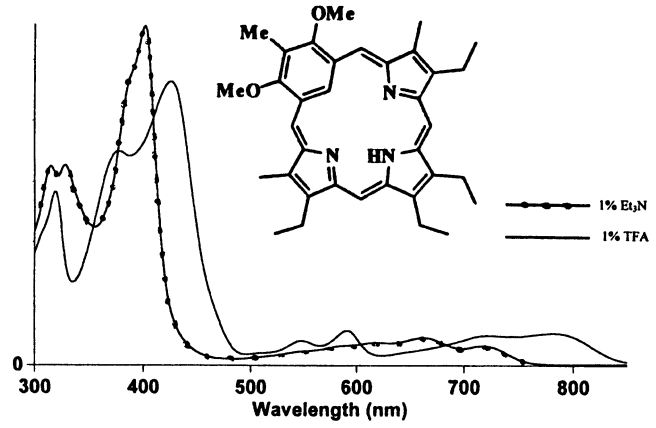

Figure 4. UV–vis spectra of dimethoxybenziporphyrin **20b** in 1% Et_3N–chloroform (dotted line) and 1% TFA–chloroform (solid line).

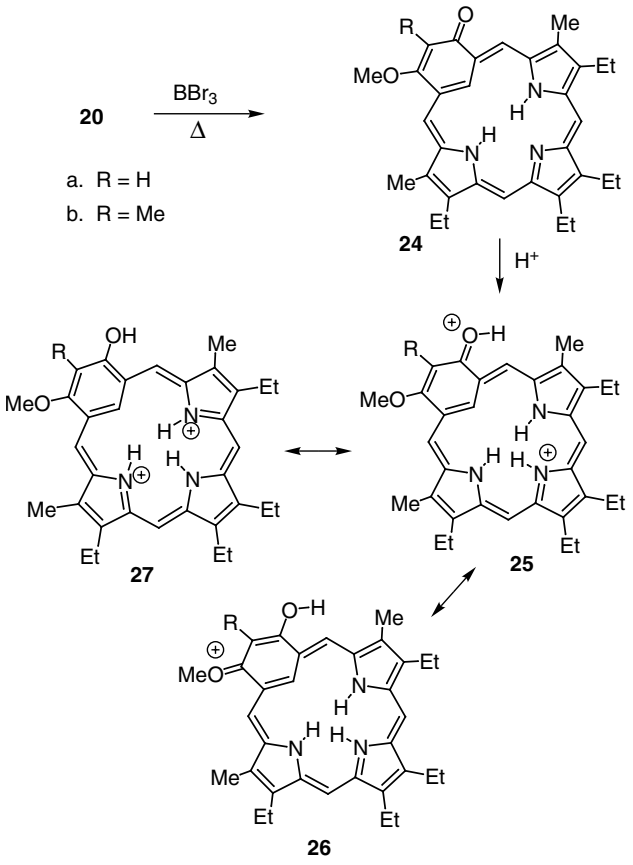

Scheme 5.

hybridized and the inability of the moieties to lie in the same plane disfavors canonical forms such as **22b** and **23b**.

Treatment of **20b** with 50 equiv. of BBr_3 at room temperature for 16 h afforded the methoxyoxybenziporphyrin **24b** in 77% yield (Scheme 5). However, prolonged reaction times and/or elevated temperatures failed to cleave the second methoxy unit. Dimethoxybenziporphyrin **20a** failed to react at all at room temperature but afforded the related oxybenziporphyrin **24a** in 62% yield on refluxing with BBr_3 in 1,2-dichloroethane under nitrogen. As expected, the new oxybenziporphyrins were fully aromatic compounds showing powerful diamagnetic ring currents in their proton NMR spectra (Fig. 5). In both cases, the internal CH was observed upfield beyond −7 ppm while the *meso*-protons appeared as a series of downfield singlets between 9.0 and 10.5 ppm. The free base for **24a** gave Soret bands at 422 and 453 nm (Fig. 6), while these absorptions were observed at 428 and 458 nm for the methyl-substituted version **24b** (Fig. 7). Addition of TFA to oxybenziporphyrin **8** led to a considerable loss of aromatic character, and it was of some interest to see whether this was also the case for the related methoxy structures. Addition of TFA to **24a** produced a dication **25a** (Scheme 5) that showed far more aromatic character than had been the case for oxybenziporphyrin **8**. In the proton NMR spectrum, the interior CH still resonated at −1.72 ppm while the *meso*-protons appeared downfield between 8.7 and 10 ppm (Fig. 8). Although the aromatic ring current is substantially reduced, resonance contributors such as **25a** and **26a** must

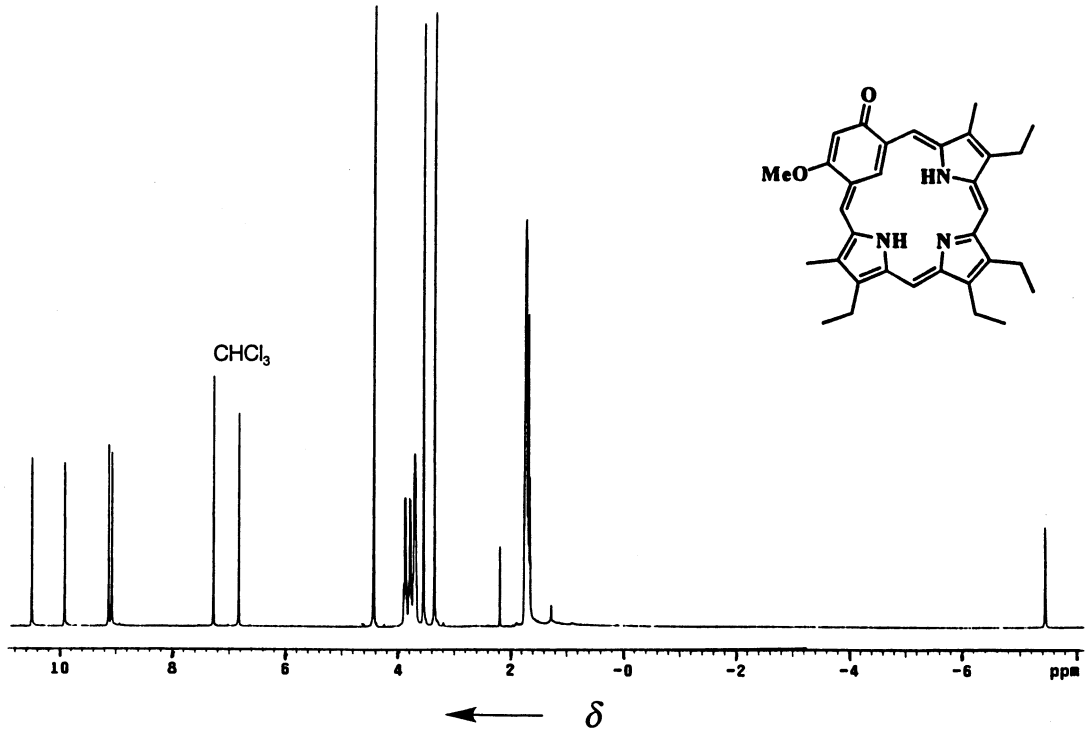

Figure 5. 400 MHz proton NMR spectrum of methoxyoxybenziporphyrin **24a** in $CDCl_3$.

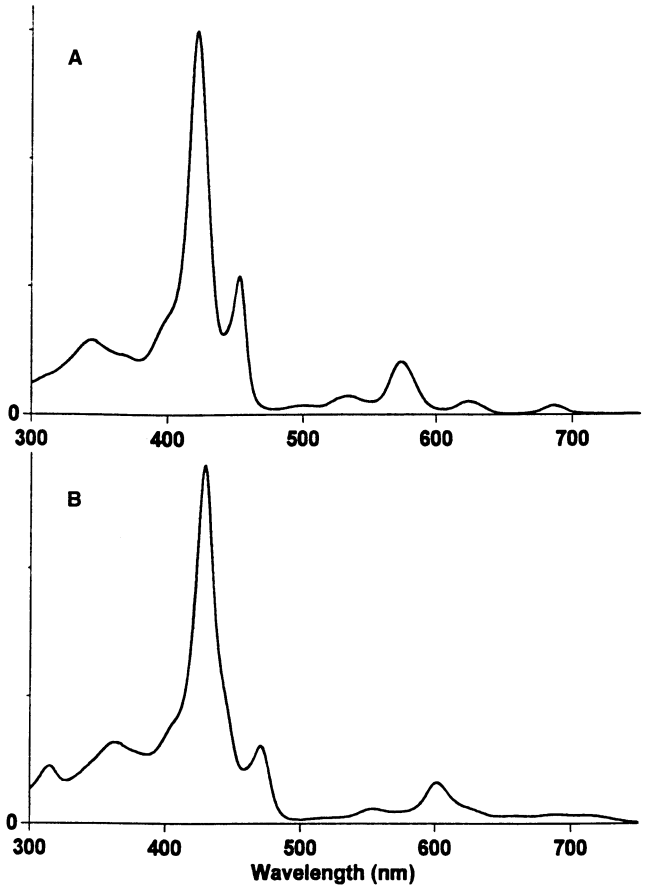

Figure 6. UV–vis spectra of methoxyoxybenziporphyrin **24a**: (A) in 1% Et_3N–chloroform (free base); (B) in 5% TFA–chloroform (dication).

significantly aid in charge delocalization and diminish the contributions from nonaromatic canonical forms such as **27a** (Scheme 5). The UV–vis spectrum for **24a** in 5% TFA–chloroform also retains a strong Soret band at 429 nm ($\log_{10} \epsilon$=5.23), confirming the retention of porphyrinoid electronic characteristics (Fig. 6). As would be expected, the methoxy unit is less effective for **24b**. In the proton NMR spectrum for **24b** in TFA–$CDCl_3$, the interior CH shifts downfield from −7.0 (for the free base) to +0.69 ppm. In addition, the *meso*-protons show up between 8.0 and 9.3 ppm. While there is clearly some residual macrocyclic ring current, the steric constraints due to the extra methyl substituent reduces the contributions from canonical forms such as **25b** and **26b**. In 5% TFA–chloroform, **24b** still shows a Soret band at 437 nm (Fig. 7), although the intensity of this electronic absorption is somewhat reduced ($\log_{10} \epsilon$=5.03). The identity of these structures was further demonstrated by carbon-13 NMR spectroscopy and mass spectrometry.

Although boron tribromide readily cleaves one of the methoxy substituents, it failed to remove the second unit. The use of trimethylsilyl iodide was also investigated but this reagent produced extensive decomposition. However, HBr was found to be effective in cleaving both of the methyl ethers from benziporphyrins **20**. Dimethoxybenziporphyrin **20a** was refluxed with HBr in acetic acid overnight; following dilution with chloroform, the mixture was washed with water and sodium bicarbonate to remove the acid. However, at this point considerable quantities of a highly insoluble material precipitated from these solutions. Initially, we believed that this material resulted from the decomposition of the starting material but further analysis demonstrated that it was in fact the desired hydroxyoxybenziporphyrin

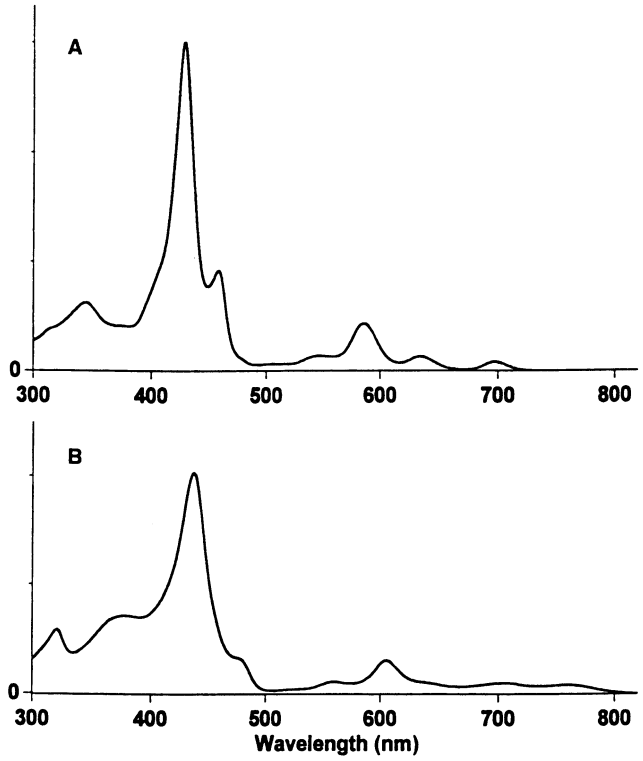

Figure 7. UV–vis spectra of methoxyoxybenziporphyrin **24b**: (A) in 1% Et_3N–chloroform (free base); (B) in 5% TFA–chloroform (dication).

17 (Scheme 6). The new porphyrinoid was isolated as a brown powder that could not be dissolved to any significant extent in organic solvents. However, addition of TFA produced the soluble dication **28** and this allowed for full spectroscopic characterization. In addition, accurate mass data for **17** could be obtained by FAB mass spectrometry. The diatropic ring current for the protonated species was larger than that exhibited for the methoxy analogue **25a**. The proton NMR spectrum of **17** in TFA–$CDCl_3$ showed the inner CH upfield at −2.4 ppm while the external *meso*-protons appeared downfield as two 2H singlets at 8.8 and 9.9 ppm (Fig. 9). The symmetry of the protonated system was also confirmed by the carbon-13 NMR spectrum which showed 5 alkyl carbons between 11 and 20 ppm, two *meso*-carbons at 93.9 and 105.4 ppm, and 9 additional resonances between 116 and 176 ppm. The UV–vis spectrum of **17** in chloroform showed a broad Soret band at 406 nm. In 5% TFA–chloroform the protonated system also showed an intense Soret absorption at 429 nm ($\log_{10} \epsilon$=5.15), providing further evidence for the aromatic nature of dication **28** (Fig. 10). The OH would be expected to be more effective than OMe in delocalizing the positive charge for the protonated species and this is borne out by the data for this species.

Dimethoxybenziporphyrin **20b** was also treated with HBr in refluxing acetic acid and a new reddish-brown product was isolated in 60% yield. However, it was immediately obvious from the spectroscopic data that the new compound was not the expected hydroxyoxybenziporphyrin. Electron impact mass spectrometry showed a molecular ion of *m/z* 523, a value that is 16 units higher than for the expected structure.

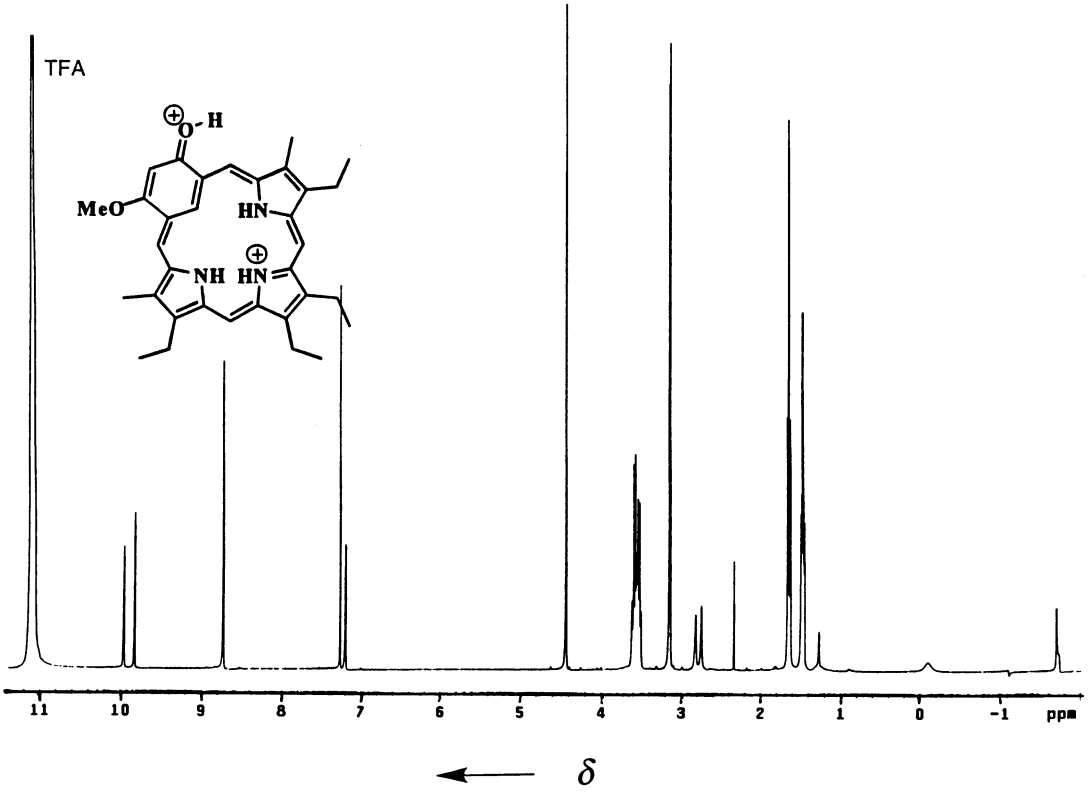

Figure 8. 400 MHz proton NMR spectrum of methoxyoxybenziporphyrin **24a** in TFA–$CDCl_3$. Although the diamagnetic ring current for the protonated porphyrinoid is reduced, the inner CH is still upfield at −1.7 ppm).

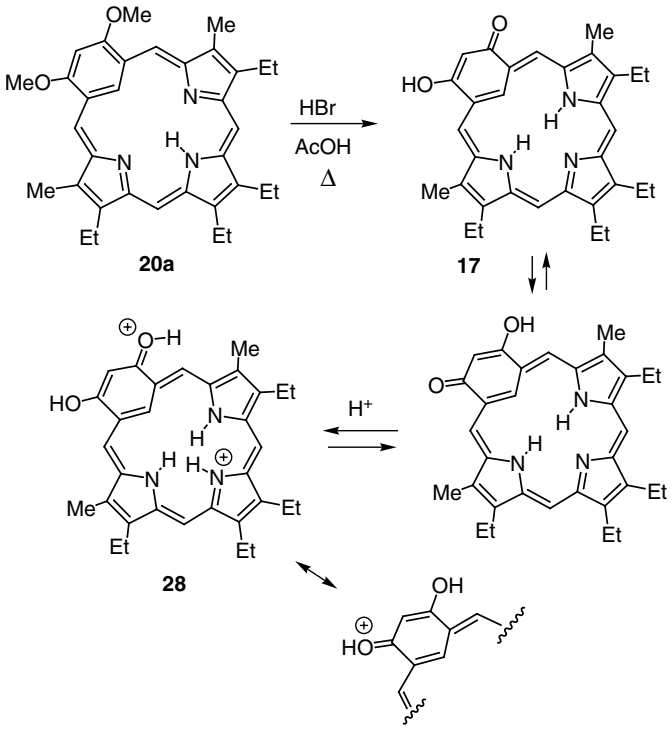

Scheme 6.

High resolution MS gave the formula $C_{33}H_{37}N_3O_3$ for this compound, demonstrating that an extra oxygen atom is present. The new structure shows a plane of symmetry by proton and carbon-13 NMR spectroscopy. The aromatic compound has a strong diatropic ring current by proton NMR spectroscopy, with the internal CH proton producing a resonance near −8.5 ppm while the external *meso*-protons gave two 2H singlets at 9.4 and 10.2 ppm (Fig. 11).

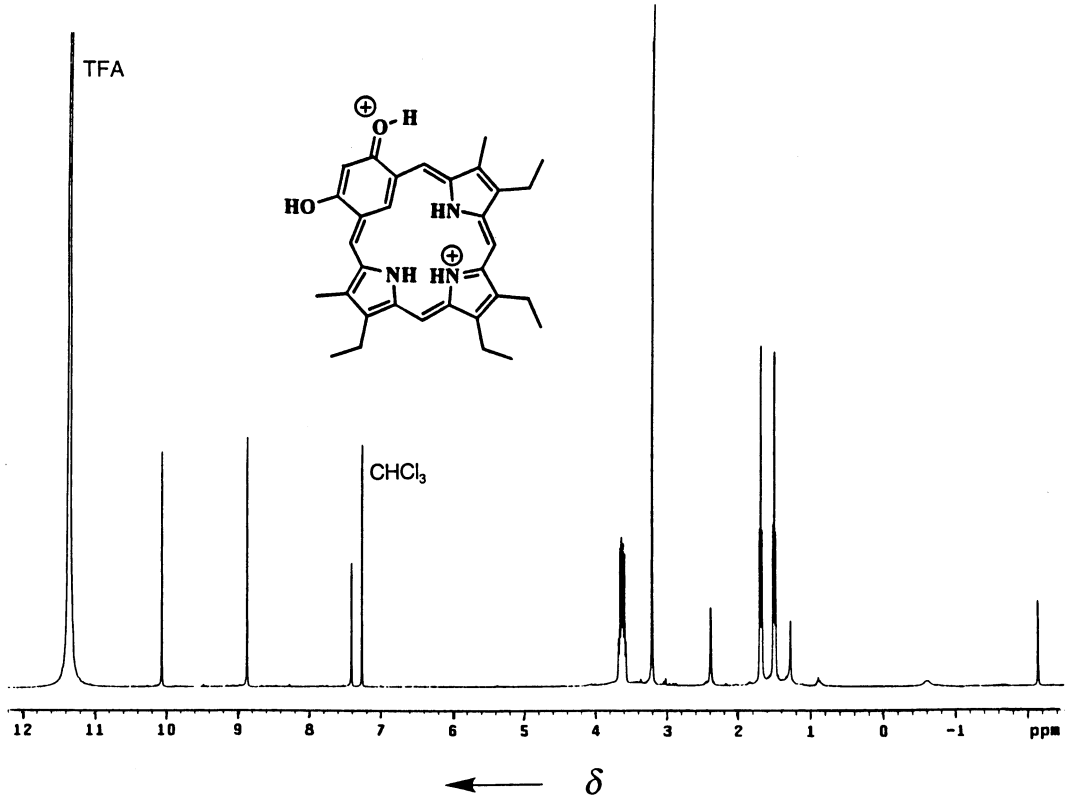

Figure 9. 400 MHz proton NMR spectrum of hydroxyoxybenziporphyrin **17** in TFA–$CDCl_3$. This diprotonated system shows a strong diamagnetic ring current due to the hydroxyl moieties enhanced ability to delocalize positive charge.

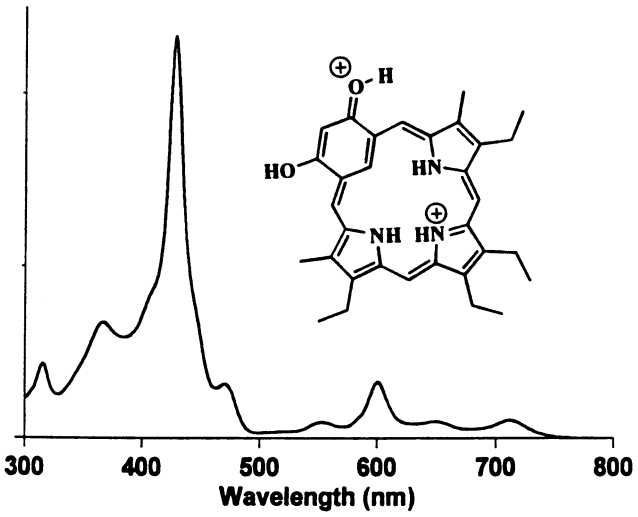

Figure 10. UV–vis spectra of hydroxyoxybenziporphyrin **17** in 5% TFA–chloroform (dication).

However, the methyl group attached to the six-membered carbocyclic ring gave a 3H singlet upfield at 1.7 ppm, suggesting the absence of an adjacent π-system. In addition, the carbon-13 NMR spectrum showed several unusual features. A resonance at 201 ppm was consistent with the presence of a ketone moiety while a signal at 86.2 ppm suggested the presence of a tertiary alcohol carbon. However, two *meso*-carbons were present at 94.7 and 103.4 together with six alkyl absorptions between 12 and 31 ppm and 8 sp^2 carbon resonances between 119 and 155 ppm. Together, these data demonstrate that the new compound is the hydroxybenziporphyrin diketone **29** (Scheme 7). The UV–vis spectrum for this novel aromatic structure shows a broad Soret band region centered on 418 nm together with three Q bands at 510, 544 and 593 nm (Fig. 12A). In the presence of TFA, the related cation **30** is formed and this shows a split Soret band at 410 and 426 nm, together with weaker absorptions at 532, 568 and 584 nm (Fig. 12B). Proton NMR spectra of **29** in TFA–$CDCl_3$ show the interior CH strongly shifted upfield to −6.45 ppm while the NH resonances are also present nearby at −5.62 and −2.64 ppm (Fig. 13). The *meso*-protons appear further downfield than was the case for the free base at 10.1 and 10.9 ppm. In this case, the ring current for the protonated system appears to be similar to the free base although some downfield shifts are evident due to the presence of the positive charge. The carbon-13 NMR for **30** also shows the presence of the carbonyl units at 202.8 ppm, the tertiary alcohol carbon at 87.2 ppm and an overall plane of symmetry.

The formation of the oxidized carbaporphyrinoid **29** is most likely due to the presence of trace amounts of bromine in the reaction mixtures, something that is virtually impossible to avoid when using hydrobromic acid. This may induce the formation of a hypobromite ester **31** from initially formed hydroxyoxybenziporphyrin **32** and subsequent attack by water would afford the observed product (Scheme 8). The presence of a methyl substituent may increase the reactivity of **32**, although the low solubility of **17** could protect this compound from further reaction.

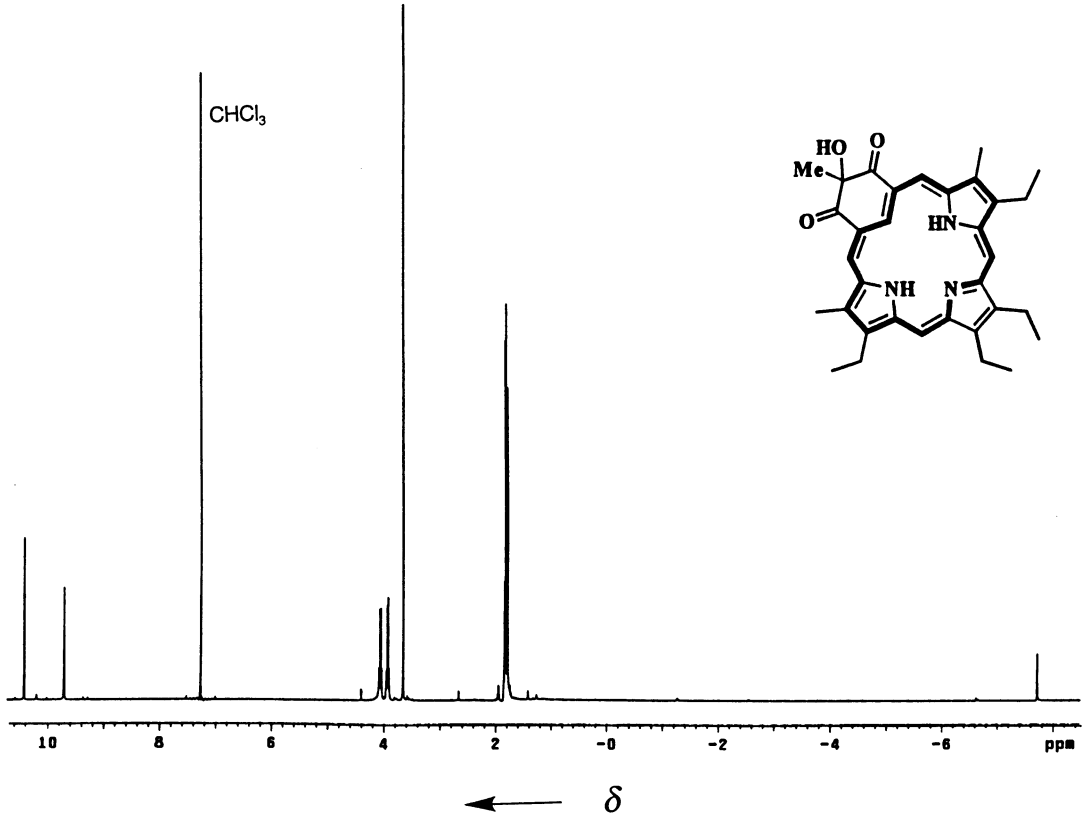

Figure 11. 400 MHz proton NMR spectrum of porphyrinoid **29** in $CDCl_3$.

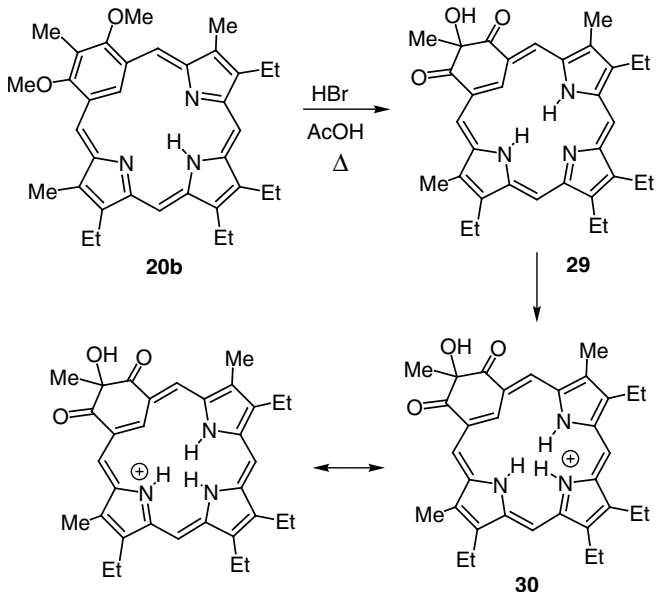

Scheme 7.

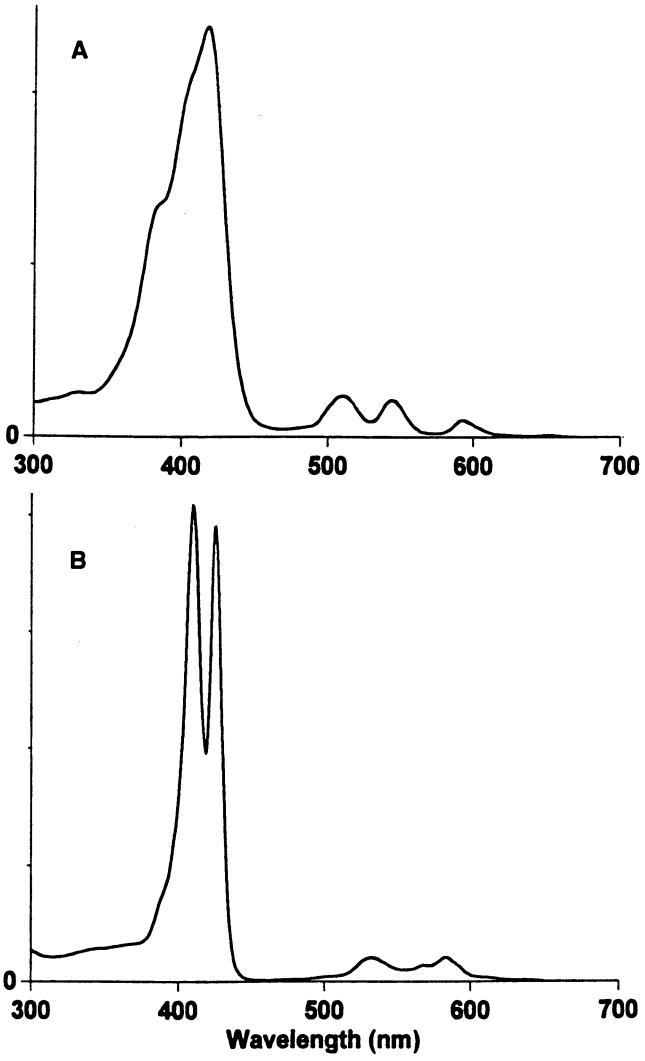

Figure 12. UV–vis spectra of porphyrinoid **29**: (A) in 1% Et_3N–chloroform (free base); (B) in 5% TFA–chloroform (cation).

3. Conclusions

Dimethoxybenziporphyrins were synthesized in excellent yields by the '3+1' methodology. The methoxy units were able to imbue the protonated structures with a degree of aromatic character to aid in charge delocalization, particularly in the case of **20a** where steric considerations were favorable. Cleavage of one methyl ether unit with boron tribromide afforded the related methoxyoxybenziporphyrins **24**. The free base structures showed carbaporphyrin-type aromatic characteristics and these were retained to a significant extent in the related dications. Treatment of **20a** with HBr in refluxing acetic acid cleaved both of the methyl ethers to give the hydroxyoxybenziporphyrin **17** while the related 3-methylbenziporphyrin oxidized to give the unusual carbaporphyrinoid diketone **29**. Both **17** and **29** are strongly diatropic by proton NMR spectroscopy and further extend the family of aromatic carbaporphyrinoid systems.

4. Experimental

4.1. General

1,3-Dimethoxybenzene, 2,6-dimethoxytoluene, *n*-butyllithium, BBr_3, DDQ and TFA were purchased from Aldrich Chemical and used without further purification. Chromatography was performed using Grade 3 neutral alumina or 70–230 mesh silica gel. Melting points were determined on a Thomas Hoover capillary melting point apparatus and are uncorrected. UV spectra were obtained on a Cary 1 Bio UV–visible spectrophotometer. NMR spectra were recorded on a Varian Gemini 400 MHz NMR spectrometer; chemical shifts were relative to chloroform at 7.27 ppm. EI and FAB mass spectral determinations were made at the Mass Spectral Laboratory, School of Chemical Sciences, University of Illinois at Urbana-Champaign, supported in part by a grant from the National Institute of General Medical Sciences (GM 27029). Elemental analyses were

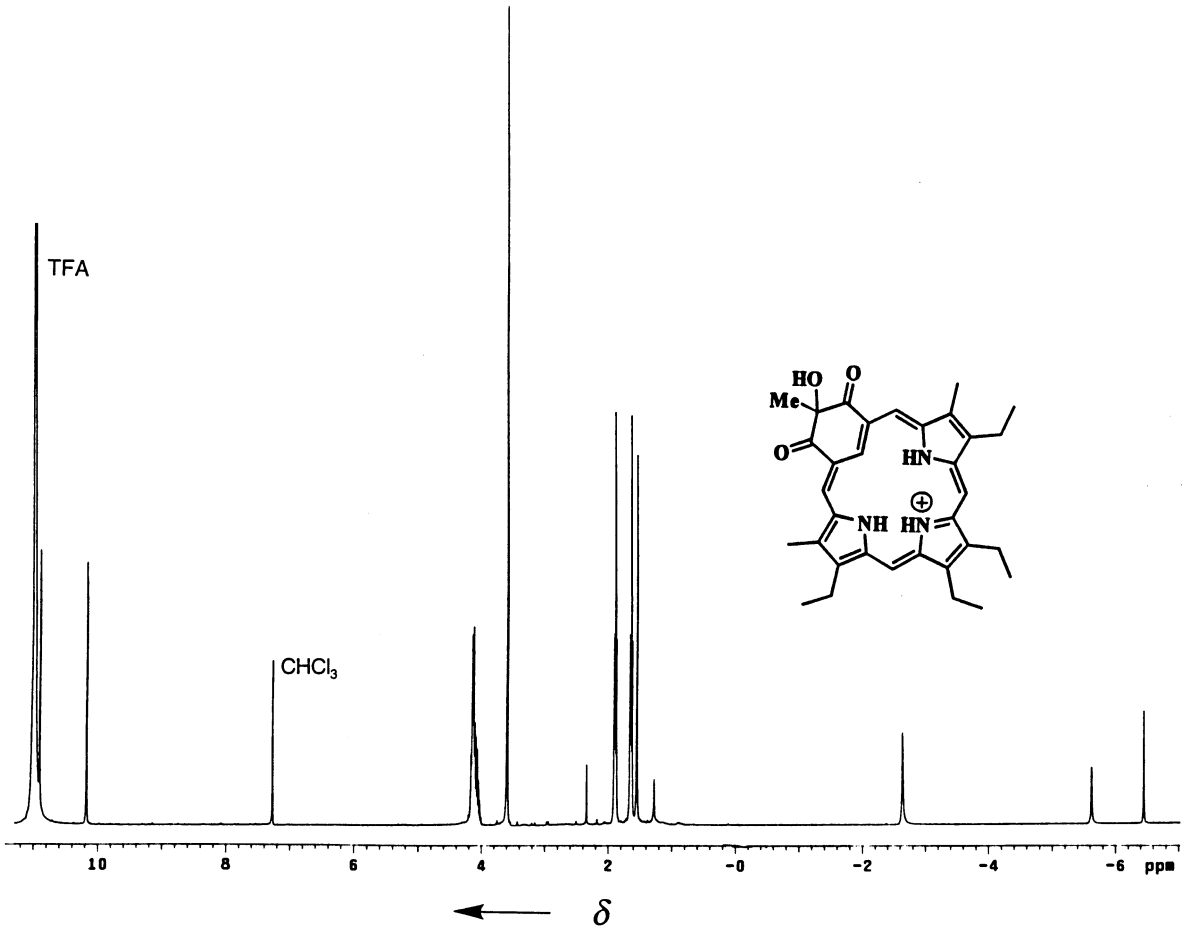

Figure 13. 400 MHz proton NMR spectrum of porphyrinoid **29** in TFA–$CDCl_3$. The protonated species retains a very strong diamagnetic ring current.

obtained from the School of Chemical Sciences Microanalysis Laboratory at the University of Illinois.

4.1.1. 9,13,14,18-Tetraethyl-2,4-dimethoxy-8,19-dimethylbenziporphyrin (20a). In a 100 mL pear shaped flask, tripyrrane dicarboxylic acid **9**[20,26] (122 mg) was stirred for 2 min in TFA (1 mL) under a nitrogen atmosphere, the solution diluted with dichloromethane (99 mL) and 4,6-dimethoxyisophthalaldehyde (53 mg) immediately added. The resulting mixture was stirred in the dark at room temperature overnight. The solution was then washed with water, 0.1% aqueous ferric chloride solution,[27] water and saturated sodium bicarbonate solution, and the solvent removed under reduced pressure (the aqueous solutions were back extracted with chloroform at each stage in the extractions). The resulting residue was recrystallized from chloroform–methanol to give the desired macrocycle (112 mg; 80%) as a purple powder, mp >260°C; UV–vis ($CHCl_3$): λ_{max} ($\log_{10}\epsilon$) 328 (4.77), 423 (4.78), 560 (3.71), 598 (3.87), 640 (3.78), 695 nm (3.56); UV–vis (1% TFA–$CHCl_3$; dication): λ_{max} ($\log_{10}\epsilon$) 319 (4.34), 356 (4.65), 443 (4.86), 561 (3.71), 607 (4.29), 679 (3.73), 745 nm (3.82); ^{1}H NMR ($CDCl_3$): δ 1.37 (6H, t), 1.45 (6H, t), 2.63 (6H, s), 2.99 (4H, q), 3.09 (4H, q), 4.23 (6H, s), 5.07 (1H, br s), 6.78 (1H, s), 7.16 (2H, s), 8.47 (2H, s); ^{1}H NMR (TFA–$CDCl_3$): δ −0.68 (1H, s), 1.19 (1H, br s), 1.46 (6H, t), 1.58 (6H, t), 3.05 (6H, s), 3.39–3.50 (8H, m), 3.68 (2H, s), 4.49 (6H, s), 7.00 (1H, s), 8.44 (2H, s), 9.60 (2H, s); ^{13}C NMR (TFA–$CDCl_3$): δ 11.40, 15.39, 16.32, 19.05, 19.21, 58.39, 93.58, 97.42, 114.02, 116.74, 118.05, 140.12, 140.62, 145.32, 146.11, 147.63, 153.03, 174.35; fab hr ms: Calcd for $C_{34}H_{39}N_3O_2$+H: 522.31205. Found: 522.3122.

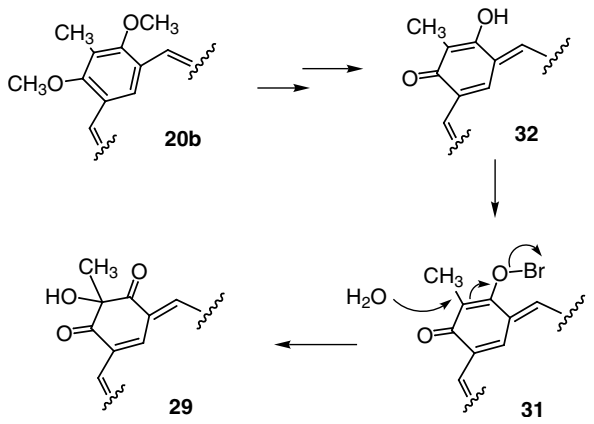

Scheme 8.

4.1.2. 9,13,14,18-Tetraethyl-4-methoxy-8,19-dimethyl-2-oxybenziporphyrin (24a). Dimethoxybenziporphyrin **20a** (40 mg) was dissolved in 1,2-dichloroethane (50 mL), BBr_3 (0.5 mL) was added and the resulting mixture placed under a nitrogen atmosphere and stirred under reflux overnight. The solution was then cooled and washed with

water, followed by saturated sodium bicarbonate solution. After removing the solvent on a rotary evaporator, the residue was chromatographed on silica eluting with 1% methanol–chloroform. Subsequent recrystallization from chloroform–methanol afforded the methoxyoxybenziporphyrin (24 mg; 62%) as dark navy blue crystals, mp 286°C; UV–vis (1% Et_3N–$CHCl_3$): λ_{max} ($\log_{10}\epsilon$) 344 (4.54), 422 (5.25), 453 (4.81), 534 (3.94), 574 (4.39), 624 (3.80), 686 nm (3.64); UV–vis (5% TFA–$CHCl_3$): λ_{max} ($\log_{10}\epsilon$) 315 (4.43), 363 (4.58), 429 (5.23), 471 (4.57), 554 (3.86), 602 (4.29), 687 nm (3.64); ^{1}H NMR ($CDCl_3$): δ −7.45 (1H, s), 1.65–1.75 (12H, m), 3.35 (3H, s), 3.55 (3H, s), 3.67–3.74 (4H, two overlapping quartets), 3.79 (2H, q), 3.87 (2H, q), 4.43 (3H, s), 6.83 (1H, s), 9.07 (1H, s), 9.13 (1H, s), 9.92 (1H, s), 10.50 (1H, s); ^{1}H NMR (TFA–$CDCl_3$): δ −1.72 (1H, unresolved doublet), −0.09 (1H, br s), 1.45–1.50 (6H, m), 1.65 (6H, t), 2.75 (1H, s), 2.82 (1H, s), 3.15 (3H, s), 3.15 (3H, s), 3.51–3.62 (8H, m), 4.44 (3H, s), 7.20 (1H, s), 8.73 (2H, s), 9.83 (1H, s), 9.96 (1H, s); ^{13}C NMR ($CDCl_3$): δ 11.70, 11.98, 17.22, 17.25, 18.36, 18.40, 19.46, 19.55, 19.81, 56.67, 93.58, 94.47, 103.77, 105.75, 105.80, 112.79, 112.83, 117.7, 123.87, 131.65, 133.29, 135.96, 136.21, 136.84, 137.59, 138.05, 139.31, 144.50, 144.77, 154.45, 155.39, 169.42, 188.73; ^{13}C NMR (TFA–$CDCl_3$): δ 11.44, 11.60, 15.63, 16.52, 19.21, 19.32, 58.50, 93.68, 93.70, 102.10, 115.44, 116.36, 117.20, 117.59, 118.06, 139.63, 139.74, 140.77, 140.81, 145.18, 145.67, 145.93, 145.96, 146.22, 151.27, 151.37, 174.79, 176.37; fab hr ms: Calcd for $C_{33}H_{37}N_3O_2$+H: 508.2964. Found: 508.2963. Anal. calcd for $C_{33}H_{37}N_3O_2\cdot H_2O$: C, 75.40; H, 7.48; N, 7.99. Found: C, 75.68; H, 6.99; N, 7.90.

4.1.3. 9,13,14,18-Tetraethyl-4-hydroxy-8,19-dimethyl-2-oxybenziporphyrin (17). Dimethoxybenziporphyrin **24a** (40 mg) was dissolved in acetic acid (35 mL). Following the addition of concentrated HBr (2 mL; 48%), the solution was heated under reflux overnight. The solution was diluted with chloroform and washed with water, followed by 10% HCl in order to generate the hydrochloride salt, and evaporated under reduced pressure. The residue was recrystallized from chloroform–hexanes to give the hydrochloride salt (24 mg; 70%) as brown crystals. The free base could be obtained by dissolving the HCl salt in methanol, adding 1–2 drops of concentrated aqueous ammonia and then filtering the solution, followed by washing with methanol to remove traces of ammonia. The free base immediately precipitates as a brown powder, mp>300°C; UV–vis (5% TFA–$CHCl_3$): λ_{max} ($\log_{10}\epsilon$) 315 (4.42), 368 (4.62), 429 (5.15), 471 (4.29), 554 (3.76), 601 (4.30), 648 (3.77), 711 nm (3.81); ^{1}H NMR (TFA–$CDCl_3$): δ −2.38 (1H, s, CH), −0.38 (1H, br s, NH), 1.47 (6H, t), 1.64 (6H, t), 2.41 (2H, s, NH), 3.16 (6H, s), 3.60 (8H, m), 6.93 (1H, s), 8.83 (2H, s), 9.91 (2H, s); ^{13}C NMR (TFA–$CDCl_3$): δ 11.69, 15.86, 16.72, 19.31, 19.35, 93.90, 105.42, 116.81, 117.20, 139.25, 140.48, 144.77, 144.95, 145.27, 150.09, 175.78; fab hr ms: Calcd for $C_{32}H_{35}N_3O_2$+H: 494.28075. Found: 494.2808.

4.1.4. 9,13,14,18-Tetraethyl-2,4-dimethoxy-3,8,19-trimethylbenziporphyrin (20b). Tripyrrane dicarboxylic acid **9**[20,26] (100 mg) and TFA (1 mL) were combined in a pear shaped flask and stirred under a nitrogen atmosphere for 2 min. The solution was diluted with dichloromethane (99 mL), 5-methyl-4,6-dimethoxyisophthalaldehyde (48 mg) was added and stirring under nitrogen continued at room temperature overnight. The solution was then washed with water, 0.1% aqueous ferric chloride solution,[27] water and saturated sodium bicarbonate solution, and the solvent removed under reduced pressure. The resulting bluish-purple solid was recrystallized from chloroform–methanol to give the dimethoxybenziporphyrin (63 mg; 55%) as bluish-purple crystals, mp 219°C; UV–vis ($CHCl_3$): λ_{max} ($\log_{10}\epsilon$) 315 (4.63), 328 (4.64), 401 (4.87), 619 (3.70), 662 (3.78), 717 nm (3.62); UV–vis (1% TFA–$CHCl_3$; dication): λ_{max} ($\log_{10}\epsilon$) 319 (4.57), 377 (4.67), 425 (4.79), 548 (3.73), 591 (3.88), 721 (3.81), 783 nm (3.85); ^{1}H NMR ($CDCl_3$): δ 1.30 (6H, t), 1.38 (6H, t), 2.46 (3H, s), 2.49 (6H, s), 2.82 (4H, q), 2.90 (4H, q), 4.03 (6H, s), 6.68 (2H, s), 7.03 (1H, s), 7.84 (2H, s), 8.55 (2H, br s); ^{1}H NMR (TFA–$CDCl_3$): δ 1.33–1.39 (12H, m), 2.39 (3H, s), 2.66 (6H, s), 2.95 (8H, q), 4.02 (6H, s), 4.25 (1H, br s), 7.04 (2H, s), 8.22 (2H, s), 9.29 (3H, vb); ^{13}C NMR ($CDCl_3$): δ 10.08, 10.66, 15.61, 16.29, 18.30, 18.65, 64.56, 92.94, 114.97, 123.34, 124.05, 125.03, 140.28, 141.64, 147.34, 156.17, 164.42, 168.25; ^{13}C NMR (TFA–$CDCl_3$): δ 10.73, 11.03, 14.68, 15.64, 18.49, 18.75, 66.34, 93.78, 107.30, 121.44, 122.22, 128.63, 140.96, 142.27, 146.12, 147.63, 151.96, 159.01, 170.47; fab hr ms: calcd for $C_{35}H_{41}N_3O_2$+H: 536.3277. Found: 536.3276. Anal. calcd for $C_{35}H_{41}N_3O_2\cdot 1/2H_2O$: C, 77.17; H, 7.77; N, 7.71. Found: C, 77.37; H, 7.73; N, 7.60.

4.1.5. 9,13,14,18-Tetraethyl-4-methoxy-3,8,19-trimethyl-2-oxybenziporphyrin (24b). In a 100 mL round bottom flask, dimethoxy-methylbenziporphyrin **20b** (30 mg) was dissolved in dichloromethane (50 mL), 1 mL of a 1 M solution of BBr_3 in dichloromethane (>50 equiv.) was added under nitrogen and the solution stirred at room temperature overnight. The solution was then washed with water, followed by saturated sodium bicarbonate solution, after which the solvent was removed under reduced pressure. The residue was chromatographed on Grade III alumina eluting with 1% methanol–chloroform. Recrystallization from chloroform–methanol afforded the oxybenziporphyrin (29 mg; 77%) as fluffy brown needles, mp 236–237°C; UV–vis ($CHCl_3$): λ_{max} ($\log_{10}\epsilon$) 344 (4.52), 428 (5.20), 458 (4.69), 546 (3.87), 586 (4.36), 634 (3.85), 698 nm (3.65); UV–vis (5% TFA–$CHCl_3$; dication): λ_{max} ($\log_{10}\epsilon$) 321 (4.49), 378 (4.58), 437 (5.04), 559 (3.76), 605 (4.21), 704 (3.71), 760 nm (3.62); ^{1}H NMR ($CDCl_3$): δ −7.03 (1H, s), 1.70–1.75 (12H, m), 2.68 (3H, s), 3.45 (3H, s), 3.49 (3H, s), 3.68–3.74 (4H, m), 3.81–3.89 (4H, m), 4.39 (3H, s), 9.09 (1H, s), 9.16 (1H, s), 9.87 (1H, s), 10.48 (1H, s); ^{1}H NMR (TFA–$CDCl_3$): δ 0.69 (1H, s), 1.40–1.44 (6H, m), 1.51–1.56 (6H, m), 2.51 (3H, s), 2.94 (3H, s), 2.96 (3H, s), 3.25–3.37 (8H, m), 4.20 (3H, s), 5.21 (1H, br s), 5.24 (1H, br s), 5.31 (1H, s), 8.05 (1H, s), 8.07 (1H, s), 9.13 (1H, s), 9.29 (1H, s); ^{13}C NMR ($CDCl_3$): δ 10.77, 11.74, 11.84, 17.16, 17.31, 18.32, 18.39, 19.50, 19.82, 63.02, 93.38, 94.87, 105.26, 105.93, 111.28, 118.72, 124.39, 126.78, 132.07, 133.82, 135.86, 136.34, 136.96, 137.69, 138.14, 139.78, 144.47, 144.92, 154.52, 155.82, 167.15, 189.60; ^{13}C NMR (TFA–$CDCl_3$): δ 9.71, 11.19, 11.34, 15.16, 15.22, 16.11, 16.14, 18.85, 19.06, 66.44, 93.50, 93.79, 109.19, 117.76, 119.60, 119.82, 120.71, 122.11, 140.73, 140.86, 141.27, 145.61, 145.84, 146.63, 147.29, 149.04, 149.45, 154.96, 155.70, 170.24, 171.69; ei hr ms: Calcd for $C_{34}H_{39}N_3O_2$:

521.3042. Found: 521.3049. Anal. calcd for $C_{34}H_{39}N_3O_2 \cdot 1/2H_2O$: C, 76.95; H, 7.59; N, 7.92. Found: C, 77.33; H, 7.26; N, 7.29.

4.1.6. 9,13,14,18-Tetraethyl-3-hydroxy-2,8,19-trimethyl-4-oxo-3,4-dihydro-2-oxybenziporphyrin (29). Dimethoxymethylbenziporphyrin **20b** (41 mg) was dissolved in acetic acid (40 mL), concentrated HBr (1 mL; 48%) was added and the solution heated to reflux under nitrogen for 90 min. The solution was cooled, diluted with chloroform and washed with water, followed by saturated aqueous sodium bicarbonate solution. The solvent removed on a rotary evaporator and the residue chromatographed on silica eluting with 50% dichloromethane–chloroform. Recrystallization from chloroform–methanol gave the hydroxy compound (22 mg; 60%) as light brownish-red crystals, mp 272°C; UV–vis (1% Et_3N–$CHCl_3$): λ_{max} ($\log_{10}\epsilon$) 418 (5.14), 510 (4.14), 544 (4.10), 593 nm (3.76); UV–vis (5% TFA–$CHCl_3$): λ_{max} ($\log_{10}\epsilon$) 410 (5.37), 426 (5.35), 532 (4.08), 568 (3.92), 584 nm (4.08); ^{1}H NMR ($CDCl_3$): δ −8.52 (1H, s, interior CH), 1.69 (3H, s), 1.76 (12H, m), 3.58 (6H, s), 3.85 (4H, m), 3.97 (4H, m), 9.39 (2H, s), 10.19 (2H, s); ^{1}H NMR (TFA–$CDCl_3$): δ −6.45 (1H, s), −5.62 (1H, s), −2.64 (2H, s), 1.55 (3H, s), 1.64 (6H, t), 1.89 (6H, t), 3.59 (6H, s), 4.06–4.17 (8H, m), 10.18 (2H, s), 10.91 (2H, s); ^{13}C NMR ($CDCl_3$): δ 11.96, 17.42, 18.56, 19.69, 19.99, 30.21, 86.17, 94.69, 103.37, 119.34, 119.92, 131.98, 136.47, 137.27, 137.40, 144.98, 154.08, 201.24; ^{13}C NMR (TFA–$CDCl_3$): δ 12.02, 16.58, 17.54, 20.00, 28.76, 87.19, 93.78, 110.67, 120.99, 129.03, 137.88, 138.64, 139.91, 141.09, 141.13, 143.18, 202.85; ei hr ms: Calcd for $C_{33}H_{37}N_3O_3$: 523.2835. Found: 523.2825. Anal. calcd for $C_{33}H_{37}N_3O_3$: C, 75.69; H, 7.12; N, 8.02. Found: C, 75.49; H, 6.68; N, 6.83.

Acknowledgements

This material is based upon work supported by the National Science Foundation under Grant No. CHE-9732054 and the Petroleum Research Fund, administered by the American Chemical Society.

References

1. Part 17: Richter, D. T.; Lash, T. D. *Tetrahedron Lett.* **1999**, *40*, 6735.
2. Medforth, C. J. In *The Porphyrin Handbook*; Kadish, K. M., Smith, K. M., Guilard, R., Eds.; Academic: San Diego, 2000; Vol. 5, pp 1–80.
3. Smith, K. M. In *Porphyrins and Metalloporphyrins*; Smith, K. M., Ed.; Elsevier: Amsterdam, 1975; Chapter 1.
4. Vogel, E.; Haas, W.; Knipp, B.; Lex, J.; Schmickler, H. *Angew. Chem., Int. Ed. Engl.* **1988**, *27*, 406.
5. Lash, T. D. In *The Macmillan Encyclopedia of Chemistry*; Lagowski, J. J., Ed.; Simon and Schuster Macmillan: New York, 1997; Vol. 3, pp 1239–1245.
6. Cyranski, M. K.; Krygowski, T. M.; Wisiorowski, M.; Hommes, N. J. R.; van, E.; Schleyer, P.; von, R. *Angew. Chem., Int. Ed. Engl.* **1998**, *37*, 177.
7. Vogel, E.; Kocher, M.; Schmickler, H.; Lex, J. *Angew. Chem., Int. Ed. Engl.* **1986**, *25*, 257.
8. Sessler, J. L.; Gebauer, A.; Vogel, E. In *The Porphyrin Handbook*; Kadish, K. M., Smith, K. M., Guilard, R., Eds.; Academic: San Diego, 2000; Vol. 2, pp 1–55.
9. Sessler, J. L.; Gebauer, A.; Vogel, E. In *The Porphyrin Handbook*; Kadish, K. M., Smith, K. M., Guilard, R., Eds.; Academic: San Diego, 2000; Vol. 2, pp 55–124.
10. Johnson, A. W. In *Porphyrins and Metalloporphyrins*; Smith, K. M., Ed.; Elsevier: Amsterdam, 1975; pp 729–754.
11. Broadhurst, M. J.; Grigg, R.; Johnson, A. W. *J. Chem. Soc. (C)* **1971**, 3681. Ulman, A.; Manassen, J. *J. Am. Chem. Soc.* **1975**, *97*, 6540. Ulman, A.; Manassen, J. *J. Chem. Soc. Perkin Trans. I* **1979**, 1066. Lash, T. D.; Motta, Y. G. *Heterocycles* **1983**, *20*, 2343. Haas, W.; Knipp, B.; Sicken, M.; Lex, J.; Vogel, E. *Angew. Chem., Int. Ed. Engl.* **1988**, *27*, 409. Vogel, E.; Rohrig, P.; Sicken, M.; Knipp, B.; Herrmann, A.; Pohl, M.; Schmickler, H.; Lex, J. *Angew. Chem., Int. Ed. Engl.* **1989**, *28*, 1651. Lash, T. D.; Armiger, Y. L. S.-T. *J. Heterocycl. Chem.* **1991**, *28*, 965. Vogel, E.; Pohl, M.; Herrmann, A.; Wiss, T.; König, C.; Lex, J.; Gross, M.; Gisselbrecht, J. P. *Angew. Chem., Int. Ed. Engl.* **1996**, *35*, 1520. Chmielewski, P. J.; Latos-Grazynski, L.; Olmstead, M. M.; Balch, A. L. *Chem. Eur. J.* **1997**, *3*, 268. Gross, Z.; Saltsman, I.; Pandian, R. P.; Barzilay, C. M. *Tetrahedron Lett.* **1997**, *38*, 2383.
12. Lash, T. D. *Synlett* **2000**, 279. Lash, T. D. In *The Porphyrin Handbook*; Kadish, K. M., Smith, K. M., Guilard, R., Eds.; Academic: San Diego, 2000; Vol. 2, pp 125–199.
13. For related studies on porphyrin isomers with inverted pyrrole rings, see: Chmielewski, P. J.; Latos-Grazynski, L.; Rachlewicz, K.; Glowiak, T. *Angew. Chem., Int. Ed. Engl.* **1994**, *33*, 779. Furuta, H.; Asano, T.; Ogawa, T. *J. Am. Chem. Soc.* **1994**, *116*, 767. Chmielewski, P. J.; Latos-Grazynski, L. *J. Chem. Soc., Perkin Trans. 2* **1995**, 503. Chmielewski, P. J.; Latos-Grazynski, L.; Glowiak, T. *J. Am. Chem. Soc.* **1996**, *118*, 5690. Ishikawa, Y.; Yoshida, I.; Akaiwa, K.; Koguchi, E.; Sasaki, T.; Furuta, H. *Chem. Lett.* **1997**, 453. Furuta, H.; Ogawa, T.; Uwatoko, Y.; Araki, K. *Inorg. Chem.* **1999**, *38*, 2676. Latos-Grazynski, L. In *The Porphyrin Handbook*; Kadish, K. M., Smith, K. M., Guilard, R., Eds.; Academic: San Diego, 2000; Vol. 2, pp 361–416.
14. Lash, T. D.; Hayes, M. J. *Angew. Chem., Int. Ed. Engl.* **1997**, *36*, 840. Lash, T. D. *Chem. Commun.* **1998**, 1683. Hayes, M. J.; Spence, J. D.; Lash, T. D. *Chem. Commun.* **1998**, 2409. For related studies, see: Lash, T. D.; Chaney, S. T. *Tetrahedron Lett.* **1996**, *37*, 8825. Lash, T. D.; Chaney, S. T. *Chem. Eur. J.* **1996**, *2*, 944. Lash, T. D.; Chaney, S. T. *Angew. Chem., Int. Ed. Engl.* **1997**, *36*, 839. Hayes, M. J.; Lash, T. D. *Chem. Eur. J.* **1998**, *4*, 508. Lash, T. D.; Richter, D. T. *J. Am. Chem. Soc.* **1998**, *120*, 9965.
15. Lash, T. D.; Romanic, J. L.; Hayes, M. J.; Spence, J. D. *Chem. Commun.* **1999**, 819.
16. Berlin, K.; Breitmaier, E. *Angew. Chem., Int. Ed. Engl.* **1994**, *33*, 1246.
17. Lash, T. D.; Chaney, S. T.; Richter, D. T. *J. Org. Chem.* **1998**, *63*, 9076.
18. Lash, T. D. *Angew. Chem., Int. Ed. Engl.* **1995**, *34*, 2533.
19. Lash, T. D. *Chem. Eur. J.* **1996**, *2*, 1197.
20. Lin, Y.; Lash, T. D. *Tetrahedron Lett.* **1995**, *36*, 9441. Lash, T. D. *J. Porphyrins Phthalocyanines* **1997**, *1*, 29.
21. Boudif, A.; Momenteau, M. *J. Chem. Soc., Perkin Trans. 1* **1996**, 1235.
22. Ghosh, A.; Wondimagegn, T.; Nilsen, H. J. *J. Phys. Chem. B* **1998**, *102*, 10459.

23. Results presented, in part, at the 216th National Meeting of the American Chemical Society, Boston, MA, August 1998 (Richter, D. T.; Lash, T. D. *Book of Abstracts*, ORGN 593) and the Symposium on Novel Porphyrinoids and their Metal Complexes—Chemistry, Photophysical Properties and Biomedical Aspects, 37th IUPAC Congress/27th Gesellschaft Deutscher Chemiker General Meeting, Berlin, Germany, August 1999 (Lash, T. D. *Book of Abstracts*—Part 1, p. 174, Abstract No. MP-2).
24. Worden, L. R.; Kaufman, K. D.; Smith, P. J.; Widiger, G. N. *J. Chem. Soc. (C)* **1969**, 227.
25. Lash, T. D.; Richter, D. T.; Shiner, C. M. *J. Org. Chem.* **1999**, *64*, 7973.
26. Sessler, J. L.; Johnson, M. R.; Lynch, V. *J. Org. Chem.* **1987**, *52*, 4394.
27. At this stage in the extraction, the chloroform and aqueous ferric chloride solutions were vigorously shaken for between 5 and 10 min to ensure complete oxidation of the initial condensation products. In cases where poor phase separation ensued, portions of brine were added and this generally took care of the problem.